JOURNAL OF CHEMICAL & ENGINEERING DATA

ARTICLE

pubs.acs.org/jced

Methane Semi-Clathrate Hydrate Phase Equilibria with Tetraisopentylammonium Fluoride

Thomas J. Hughes*,† and Kenneth N. Marsh‡

†School of Chemical and Mechanical Engineering M050, University of Western Australia, 35 Stirling Highway, Crawley 6009, Western Australia, Australia

‡Department of Chemical and Process Engineering, University of Canterbury, Christchurch 8140, New Zealand

Supporting Information

ABSTRACT: Semiclathrate hydrates (SCH), containing organic salts, typically tetraalkylammonium based, have vacant cages that can be occupied by gas molecules, and some exhibit melting temperatures at atmospheric pressure of greater than 300 K. The aim of this work was to investigate the *p*, *T* phase equilibria of the SCH former tetraisopentylammonium fluoride, specifically at a composition of $(i\text{-}C_5H_{11})_4NF \cdot 38H_2O$, in the presence of methane. Dissociation temperatures were measured at pressures from (0.57 to 26.7) MPa. At 26.7 MPa the dissociation temperature of the SCH increased to about 320 K about 15 K higher than the melting point observed by McMullan and Jeffrey (*J. Chem. Phys.* **1959**, *31*, 1231−1234) at atmospheric pressure. We also observed that at atmospheric pressure the SCH can enclathrate methane up to its melting point, this being over 110 K higher than the equilibrium dissociation temperature of methane hydrate at the same pressure. At 10 MPa the SCH dissociation temperature was about 29 K higher than the methane hydrate dissociation temperature. The transport of natural gas over maritime distances greater than 1000 km is most often achieved by cryogenic liquefaction to produce liquefied natural gas (LNG) for tanker shipment. Natural gas hydrates have been suggested as an alternative storage method to LNG tanker transportation by Berner (The Marine Transport of Natural Gas In Hydrate Form. *Proceedings of the Second International Offshore and Polar Engineering Conference*, San Francisco, CA, June 14−19, 1992; pp 636−643) and Gudmundsson and Børrehaug (*Petrol. Rev.* **1996**, *50*, 232−235). At atmospheric pressure natural gas hydrates are stable only at low temperature, less than 240 K. Semiclathrate hydrates are a possible methane storage alternative to natural gas hydrates.

INTRODUCTION

Hydrate forming tetraalkylammonium salts were discovered by Fowler et al. in the 1940s.[1] The structures of these hydrates, as well of those of other peralkylonium salts, were investigated by X-ray crystallography first by Jeffrey, McMullan, and co-workers[2−7] and more recently by other authors.[8−14] These investigations revealed hydrogen bonded cages, similar to gas clathrate hydrates; however, the charged centers of the cation and anion replaced water at some lattice sites and the alkyl chains of the salt occupied larger cages of the structures. These larger cages were either tetrakaidecahedral (with twelve pentagonal faces and two hexagonal faces, in short hand $5^{12}6^2$), pentakaidecahedral ($5^{12}6^3$), or hexakaidecahedral ($5^{12}6^4$), and between these large cages smaller dodecahedral (5^{12}) cages filled space. The breaking of the water lattice by the salt ions lead Davidson[15] to introduce the term "semi-clathrate hydrate" (SCH). The structural studies also revealed that each peralkylonium salt can form several different SCH structures with differing hydration numbers. The reviews of Davidson,[15] Dyadin and Udachin,[10] and Jeffrey[16] list many perkalkylonium salt hydrate hydration numbers, their unit cell size, and space group as well as cage structure. Lipkowski et al.[12] has shown that tetraisopentylammonium fluoride, $(i\text{-}C_5H_{11})_4NF$, the SCH form used in this work, can form SCH structures with at least three different hydration numbers (27, 32.8, and 38); the structure that forms is dependent on the ratio of salt to water in the solution and the temperature. Lipkowski et al. produced a *T*, *x* phase diagram showing the stable regions for each hydration number but also noted metastability effects. In the region of the phase diagram where $(i\text{-}C_5H_{11})_4NF \cdot 27H_2O$ is the most stable SCH, they noted that "$[(i\text{-}C_5H_{11})_4NF \cdot 38H_2O]$ was observed repeatedly, which was presumably due to kinetic difficulties in the formation of the hydrate $[(i\text{-}C_5H_{11})_4NF \cdot 27H_2O]$".

The potential for small gas molecules to fill the 5^{12} cages, as they do in gas clathrate hydrates,[17] was first noted by McMullan et al.[7] who observed gas, revealed by chromatography to be air, bubbling from melting crystals of tetra-*n*-butylammonium fluoride SCH. Similar observations were made by Jeffrey[16] and Davidson.[15] Stupin and Stravitnaya[18,19] showed that sulfur dioxide could be adsorbed on SCHs. Shimada et al.[20] and Kamata et al.,[21] however, provided the first evidence that SCH could enclathrate other small molecules, such as methane and nitrogen, that typically occupy the 5^{12} cages of natural gas hydrates. In addition, Shimada et al.[20] and Kamata et al.[21,22] showed that SCH may be used in gas separation.

Special Issue: Kenneth N. Marsh Festschrift

Received: June 2, 2011
Accepted: August 3, 2011
Published: August 22, 2011

Table 1. Potential Methane Storage Capacities and Structural Details of the SCH and Other Hydrates

hydrate	T_m[a]/K	r[b]	$w_{CH_4,max}$[c]/%	ρ_{CH_4}[d]/kg·m^{-3}	ρ_{hyd}[e]/kg·m^{-3}	cage structure[f]
$(i\text{-}C_5H_{11})_4NF\cdot 38H_2O$[g]	304.4 (305.6[i])	3	4.6	49	1070	$4\times5^{12}6^2$, $4\times5^{12}6^3$ (salt alkyl chains) + 6×5^{12}, $Z=2$
		2[h]	3.1	33	1054	
$(i\text{-}C_5H_{11})_4NF\cdot 32.8H_2O$[i]	304.6	2	3.4	38	1100	$16\times5^{12}6^2$, $4\times5^{12}6^3$ (salt alkyl chains) + 10×5^{12}, $Z=5$[j]
$(i\text{-}C_5H_{11})_4NF\cdot 27H_2O$[i]	307.8	1	2.0	22[k]	1101	$16\times4^25^96^37^1$ (salt alkyl chains) + $4\times4^45^4$, $Z=4$
$(n\text{-}C_4H_9)_4NBr\cdot 38H_2O$[l]	283.1	3	4.6	50	1095	$4\times5^{12}6^2$, $4\times5^{12}6^3$ (salt alkyl chains) + 6×5^{12}, $Z=2$
		2[h]	3.1	33	1078	
$(n\text{-}C_4H_9)_3PO\cdot 34.5H_2O$[m]	280.3	3.5	6.3	65	1030	$4\times5^{12}6^2$, $4\times5^{12}6^3$, $4\times5^{12}6^4$ (salt alkyl chains) + 14×5^{12}, $Z=4$
$THF\cdot 17H_2O$[n]	277.3	2	7.8	82	1048	$8\times5^{12}6^4$ (THF) + 16×5^{12}
$CH_4\cdot 6H_2O$	193.2[o]		12.9	121	935[p]	2×5^{12}, $6\times5^{12}6^2$
self-preserved $CH_4\cdot 6H_2O$[q]	267		6.5	60		2×5^{12}, $6\times5^{12}6^2$
liquid CH_4[r]	111.7		100	422		

[a] Melting or dissociation temperature of the hydrate or normal boiling temperature for liquid methane. [b] Ratio of cages not filled by alkyl chains per salt molecule, or for THF hydrate the ratio of unoccupied cages per molecule of THF. [c] Maximum mass fraction of methane assuming full occupancy of cages except where noted otherwise. [d] Mass of methane per unit volume. [e] Density of hydrate filled with methane assuming no expansion of the lattice due to methane inclusion except from $CH_4\cdot 6H_2O$. [f] Cage structure of the hydrates per unit cell where Z is the number of salt molecules per unit cell. [g] From Feil and Jeffrey[4] and/or McMullan and Jeffrey[6] unless otherwise noted. [h] Wang et al.'s[14] crystal structure for $(i\text{-}C_5H_{11})_4NBr\cdot 38H_2O$ indicates that one-third of the 5^{12} cages are too distorted for methane to occupy and that these cages may be occupied by water molecules. Calculations on this line assume that this is the case for this isostructural SCH. [i] Data from Lipkowski et al.[12] unless otherwise noted. [j] Cage structure assumed to be identical to that for $(n\text{-}C_4H_9)_4NF\cdot 32.8H_2O$[7] as they share the same crystallographic space group and similar unit cell dimensions. [k] We estimate that the 4^45^4 is in fact too distorted to enclathrated methane molecules (see Supporting Information); however, for this calculation we have assumed that this cage can enclathrate methane. [l] Data from Shimada et al.[13] except melting temperature from Oyama et al.[50] [m] Data from Alekseev et al.[9] except the melting temperature from Dyadin and Udachin[10] (Figure 18b therein). [n] Density estimated from pure THF hydrate lattice parameter of Tse[52] assuming full occupation of small cages by methane molecules (lattice expansion neglected). Dissociation temperature from Handa et al.[53] [o] Dissociation temperature from Fallabella and Vanpee.[42] [p] Calculated using CSMGem. [q] Assumed methane hydrate composition and anomalous self-preservation temperature from Stern et al.[43] Mass fraction of methane estimated assuming 50 % dissociation given a 1 month transport time (refer Figure 1 of Stern et al.) [r] Calculated in Refprop.[54]

As part of gas storage studies and separation studies, many measurements of the p, T phase stability of SCH at elevated pressure and temperatures higher than their atmospheric pressure melting temperature have been recently reported. Measurements of methane SCH p, T phase stability have been made with tetra-*n*-butylammonium bromide, $(n\text{-}C_4H_9)_4NBr$, by Li et al.,[23] Arjmandi et al.,[24] Mohammadi and Richon,[25] Sun and Sun,[26] and Acosta et al.[27] In addition, measurements have been made with tetra-*n*-butylammonium chloride by Makino et al.[28] For the methane + tetraisopentylammonium bromide system Wang et al.[14] present p, T phase measurements that investigated the effect of pressure on the melting temperature of the SCH on a polymer support (no measurements were tabulated or plotted at temperatures above the atmospheric pressure melting temperature of the SCH; however, a p, T point at about 315 K and 10.1 MPa can be estimated from Figure 3 of their work). No p, T phase stability of SCH forming tetraisopentylammonium salts at elevated pressure and temperatures higher than their atmospheric pressure melting temperature have been reported. A table of p, T phase stability measurements listing other gases, SCH forming salts, and authors is included in the Supporting Information. An important observation from this body of work was made by Hashimoto et al.,[29] who completed four sets of p, T phase stability measurements on the system $H_2 + (n\text{-}C_4H_9)_4NBr + H_2O$ at different mass fractions of the salt. They noted that each p, T curve coincided at atmospheric pressure with the atmospheric pressure T, x phase diagram for $(n\text{-}C_4H_9)_4NBr + H_2O$, indicating that the most stable SCH at atmospheric pressure would also form the most stable SCH at elevated pressures. However, this does not appear to be true for larger gas molecules. Deschamps and Dalmazzone[30] compared the atmospheric pressure $(n\text{-}C_4H_9)_4NBr + H_2O$ T, w phase diagram data to their measurements under 2 MPa of CO_2 and (12 and 25) MPa of N_2. The most stable SCH at atmospheric pressure for this system is $(n\text{-}C_4H_9)_4NBr\cdot 24H_2O$ (w = 0.4271);[31] however, Deschamps and Dalmazzone's data at elevated pressure indicate a temperature maxima somewhere in the range w = (0.25 to 0.35), indicating another SCH structure with a higher hydration number is the most stable at elevated pressure. These results suggest that at elevated pressure the size of the gas molecule is a determining factor in the SCH structure that is formed.

Over maritime distances of over 1000 km transport of natural gas is most often achieved by cryogenically liquefying the gas and shipping it as liquefied natural gas (LNG). Berner[32] first suggested that natural gas hydrates (NGHs) might be a suitable alternative to LNG for shipment and considered the technical challenges of hydrate production and transport. Gudmundsson and co-workers[33−39] proposed that NGH shipment might be economically attractive alternative to LNG particularly for "stranded" natural gas reserves. These stranded reserves are usually considered either too small or too distant from markets to be transported by pipeline or justify the costs of an LNG production plant. Following the discovery of the so-called "hydrate self-preservation effect" by Yakushev and Istomin,[40]

Gudmundsson et al.[41] demonstrated that natural gas hydrates could remain practically stable at atmospheric pressure when refrigerated to 258 K. This is much higher than the dissociation temperature of methane hydrate at atmospheric pressure of 193.2 K measured by Fallabella and Vanpee.[42] Stern et al.[43] also investigated the hydrate self-preservation effect and showed that after 1 month at 267 K 50 % of the methane was still stored in hydrate. The commercialization of NGH tanker shipment is still under consideration, particularly by a group of nine Japanese companies lead by Mitsui.[44] A methane storage alternative to NGH may be SCHs. SCH have the advantage that they are in general stable at higher temperatures. In Table 1 the estimated methane storage capacities of $(i\text{-}C_5H_{11})_4NF\cdot(27, 32.8$ and $38)H_2O$, $(n\text{-}C_4H_9)_4NBr\cdot 38H_2O$, tetrahydrofuran (THF) hydrate, methane hydrate, self-preserved methane hydrate, and liquid methane are compared. Details of the cage structure and melting or dissociation temperatures for each hydrate are also included (for liquid methane the atmospheric boiling temperature is listed). The storage density of methane (mass of methane per unit volume) is lower in the hydrates than liquid methane; however, the hydrates are stable at considerably higher temperature. Assuming a transport time of 1 month at 267 K a self-preserved methane hydrate would store about 60 $kg\cdot m^{-3}$ from the data of Stern et al.[43] From X-ray crystallography Wang et al.[14] showed that one-third of 5^{12} cages in $(i\text{-}C_5H_{11})_4NBr\cdot 38H_2O$ are likely too distorted to fit methane molecules; as $(i\text{-}C_5H_{11})_4NF\cdot 38H_2O$ and $(n\text{-}C_4H_9)_4NBr\cdot 38H_2O$ are isostructural to this SCH, one-third of their 5^{12} cages are also likely to be too distorted to accommodate methane. This means that there are only two occupiable 5^{12} cages per salt molecule and the maximum storage density of methane is about 33 $kg\cdot m^{-3}$ (assuming both 5^{12} cages are occupied) for both of these SCH. Alekseev et al.'s[9] crystallography data for the tri-*n*-butylphosphine oxide SCH $(n\text{-}C_4H_9)_3PO\cdot 34.5H_2O$ indicate 3.5 5^{12} cage molecules of salt. If methane can occupy all these cages, a methane storage density of 65 $kg\cdot m^{-3}$ could be achieved (however, the distortion of these cages has not been assessed to determine whether methane can occupy all cages in this structure). If all the 5^{12} cages of the structure II THF hydrate are filled with methane, a storage density of 82 $kg\cdot m^{-3}$ would result, this is higher than for any of the SCH. To determine the feasibility of using an SCH as an alternative to NGH, a full economic analysis would need to be conducted and is beyond the scope of this work. An economic advantage of the use of an SCH could be reduced or no refrigeration costs in the transport of the methane or the production of the storage material.

EXPERIMENTAL SECTION

Materials. Methane was supplied by Southern Gas Services from Linde Gas, U.K. Ltd., with a mole fraction purity of 0.999 75. The purities and suppliers of other chemicals are listed in Table S1 of the Supporting Information.

Tetraisopentylammonium bromide $[(i\text{-}C_5H_{11})_4NBr]$ was prepared by the Menshutkin reaction following the method of Lipkowski et al.[12] Triisopentylamine and isopentyl bromide were refluxed in acetonitrile under nitrogen for about 28 h. The solvent was evaporated by heating under vacuum, and the crystals were then dissolved in warm ethyl acetate. The $(i\text{-}C_5H_{11})_4NBr$ was recrystallized overnight at 275 K. The crystals were then filtered from the solution and the process of recrystallization from fresh ethyl acetate was repeated twice. The crystalline mass was then dried in a vacuum oven at 313 K until a constant mass was achieved. Further purification was performed by dissolving the crystals in deionized water and crystallizing the semiclathrate hydrate of $(i\text{-}C_5H_{11})_4NBr$, followed by drying to constant mass in a vacuum oven at 313 K. An aqueous solution of AgF was freshly prepared from BaF_2 and Ag_2SO_4. The AgF solution was added in excess to $(i\text{-}C_5H_{11})_4NBr$ solution, and the precipitated AgBr was filtered off. The $(i\text{-}C_5H_{11})_4NF$ SCH was then crystallized from the solution over several days at 275 K. The SCH was filtered off and dissolved in fresh water and recrystallized. The purity of the SCH was assessed by ^1H NMR. The $(i\text{-}C_5H_{11})_4NF$ SCH was dissolved in tetradeuterated methanol. No amine, acetone, or ethyl acetate peaks were observed in the spectra. This spectra are presented as Figure S1 in the Supporting Information.

The mole fraction of $(i\text{-}C_5H_{11})_4NF$ in solution for *p*, *T* phase measurements was fixed by crystallizing a SCH of known hydration number. The hydration number of 38 was desired as its SCH structure contains the highest number of unoccupied (5^{12}) cages per mole of salt (however, as discussed above, Wang et al.[14] have observed that one-third of the 5^{12} cages in the related $(i\text{-}C_5H_{11})_4NBr$ SCH are distorted and some of these cages are occupied by water molecules). A dilute aqueous solution of $(i\text{-}C_5H_{11})_4NF$ was prepared by dissolving SCH crystals in warm deionized water. The salt mass fraction in the solution was determined by Karl Fischer (KF) water content titration. The volumetric Karl Fischer titrator was calibrated with a 1 % mass fraction water standard. The $(i\text{-}C_5H_{11})_4NF$ solution concentration was determined by adding a small amount of the solution to methanol that had been analyzed for water content by KF titration. A known mass of the dilute $(i\text{-}C_5H_{11})_4NF$ solution was injected by syringe into a sealed septum bottle containing a known mass of methanol. The mass fraction of water in the $(i\text{-}C_5H_{11})_4NF$ solution was calculated by comparing the water content of methanol and methanol + $(i\text{-}C_5H_{11})_4NF$ solution samples. The mass fraction of $(i\text{-}C_5H_{11})_4NF$ in the dilute solution was calculated as 0.031 ± 0.001, corresponding to a mole fraction of 0.0018 ± 0.0001. This composition is well within the region of $(i\text{-}C_5H_{11})_4NF\cdot 38H_2O$ formation in the phase diagram of the $(i\text{-}C_5H_{11})_4NF$ + water system presented by Lipkowski et al.[12]

The SCH was crystallized from the dilute solution of $(i\text{-}C_5H_{11})_4NF$ over several days at 275 K. The SCH was vacuum filtered and gently pressed between two sheets of absorbent paper to reduce the remaining liquid. The hydration number of the SCH was determined by KF titration. SCH samples of known mass were dissolved in a septum bottle containing a known mass of methanol that had been analyzed for water content by KF titration. Dry nitrogen was flushed through the top of the septum bottle while the sample was added so that the methanol could not absorb more water from the air. The water mass fractions both in the methanol and in the methanol + dissolved $(i\text{-}C_5H_{11})_4NF$ SCH sample were used to calculate the hydration number of the SCH, found to be 38.3 ± 0.7 (or a mass fraction, *w*, of the salt of 0.315 ± 0.004). This hydration number compares well with the structural hydration number for $(i\text{-}C_5H_{11})_4NBr$ SCH of 38.2 measured by Wang et al.[14]

Measurements. In this work the isochoric pressure search method was used to measure the *p*, *T* phase equilibria. This method has been commonly used for measuring gas hydrate *p*, *T* phase equilibrium data[17,45] and has also been recently used in SCH gas hydrate *p*, *T* phase equilibrium data studies.[24−27,46−49]

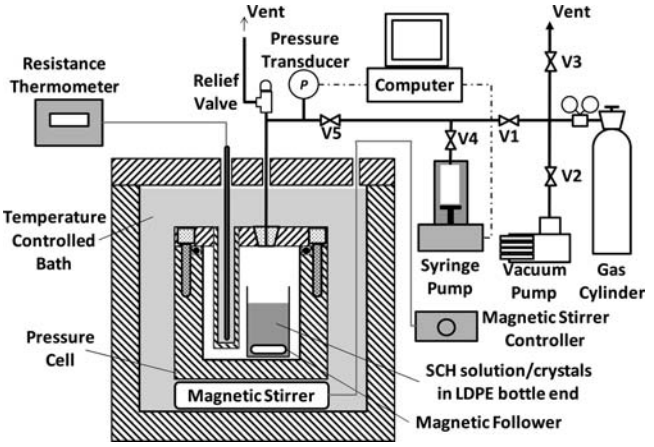

Figure 1. Apparatus for p, T tetraisopentylammonium fluoride solution + methane semiclathrate hydrate phase equilibria measurements.

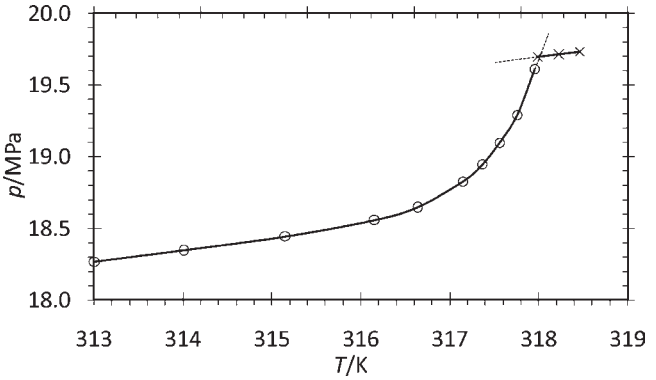

Figure 2. Example of the p, T measurements to determine a tetraisopentylammonium fluoride aqueous solution [$(i\text{-}C_5H_{11})_4NF$, w = 0.315] + methane three-phase p, T SCH + L + V value: ○, measurements with solid phase present; ×, measurements after solid phase disappearance. Determination of the point T = (318.00 ± 0.02) K and p = (19.680 ± 0.004) MPa.

A simplified diagram of the experimental apparatus is shown in Figure 1. The measurements were conducted using a custom built 94 mL stainless steel high pressure cell (maximum p = 35 MPa). A magnetic follower and 19.3046 g of the SCH were loaded inside a small low density polyethylene (LDPE) cutoff bottle (of diameter about 25 mm and height about 60 mm) and placed inside the pressure cell (the purpose of this bottle was to protect the cell from potential corrosion). The pressure cell was sealed and placed within the temperature controlled bath on top of a submersible magnetic stirrer (specifications and manufacturers of the equipment used in measurements is included in Table S4 of the Supporting Information). The temperature inside the cell was monitored with a PRT-100 Ω probe (DSIR thermo RT200 platinum resistance thermometer, uncertainty, u = 0.01 K, calibrated by Industrial Research Limited's Measurement Standards Laboratory of New Zealand traceable to ITS-90), placed inside the pressure cell's thermowell, and the pressure was monitored using a piezoelectric quartz pressure transducer (Paroscientific 9000-6K-101, u_r = 0.01 % for p > 1.4 MPa, u = 0.14 kPa for $p \leq$ 1.4 MPa, NIST traceable calibration performed by the manufacturer).

The bath was initially set to a temperature of 293.15 K. Methane was purged into the cell from a cylinder to a pressure of about 0.5 MPa. The system was then vented down to close to atmospheric pressure and was vacuum pumped down to 0.013 MPa. This purging process was thrice repeated. As $(i\text{-}C_5H_{11})_4NF$ SCHs are still solids at 293.15 K and potentially contain enclathrated air, a further purging process was repeated at a temperature higher than the melting temperature. The cell was filled with methane to about 1 MPa and heated to 313.15 K with the magnetic stirrer turned on. The bath temperature was lowered to 273.15 K, and the gas was vented to close to atmospheric pressure followed by vacuuming to 0.013 MPa. This process was repeated once more.

The bath temperature was then set to 283.15 K, and the gas was compressed in to the cell to about 20 MPa with the syringe pump. After pressurization, valve 5 was closed to limit the volume of gas outside the temperature controlled bath. Initially, efforts focused on measuring the storage capacity of methane in the SCH. The pressure of methane dropped very slowly, and after 4 weeks the pressure stabilized at p = 19.4 MPa. From the cell volume and pressure the estimated composition was $1.58CH_4 \cdot (i\text{-}C_5H_{11})_4NF \cdot 38.3H_2O$. Wang et al.[14] suggests that one-third of the 5^{12} cages in the $(i\text{-}C_5H_{11})_4NBr \cdot 38H_2O$ SCH are too distorted to fit methane molecules and some of these cages may be occupied by water molecules, referred to as type B cages in their work. This means that only two out three 5^{12} cages, referred to by Wang et al. as type A cages, per $(i\text{-}C_5H_{11})_4N^+$ ion can be occupied. This indicates that an occupancy factor of about 80 % was achieved in the type A 5^{12} cages. After this measurement was completed, p, T phase boundary measurements by the isochoric pressure search method were started. McMullan and Jeffrey[6] measured the melting temperature of $(i\text{-}C_5H_{11})_4NF \cdot 38 H_2O$ as (304.4 ± 0.2) K (note that McMullan and Jeffrey list a hydration number of a ≈40, which was later determined to be 38 crystallographically by Feil and Jeffrey[4]). The melting temperatures of $(n\text{-}C_4H_9)_4NBr \cdot$(26 and 38)$H_2O$ are listed by Oyama et al.[50] as (285.2 and 283.1) K, respectively. As a first approximation from these melting points it was estimated the SCH + aqueous solution + vapor (SCH + L + V) phase boundary for $(i\text{-}C_5H_{11})_4NF$ would be approximately 20 K higher than for $(n\text{-}C_4H_9)_4NBr$. The p, T phase data of Li et al.[23] and Arjmandi et al.[24] for $(n\text{-}C_4H_9)_4NBr$ + water + methane were used to estimate approximate dissociation conditions and the initial starting pressure of methane. Isothermal steps were begun approximately 5 K below the estimated dissociation conditions. For each isothermal step the temperature of the bath was held constant for between (20 and 28) h to allow the pressure to equilibrate. Initially, the bath temperature was raised in steps between (1 and 2) K; however, when a steeper rise in pressure between steps was observed, indicating the start of methane SCH dissociation, smaller steps of between (0.1 and 0.5) K were taken. The SCH + L + V phase equilibrium was taken as the intercept in the p, T plot, as shown in Figure 2, which is an example of the measurements taken for a single p, T SCH + L + V phase equilibrium point.

The highest melting temperature SCH of $(i\text{-}C_5H_{11})_4NF$ has a hydration number of 27 with a melting temperature according to Lipkowski et al.[12] of 307.8 K. Although it was noted as more stable, Lipkowski et al. suggested that the SCH with a hydration number of 38 was kinetically favored; hence the SCH was reformed in the pressure cell by lowering the bath temperature to between (273 and 283) K and then heating to 309 K. This was assumed to remove the structures of the SCH that cannot

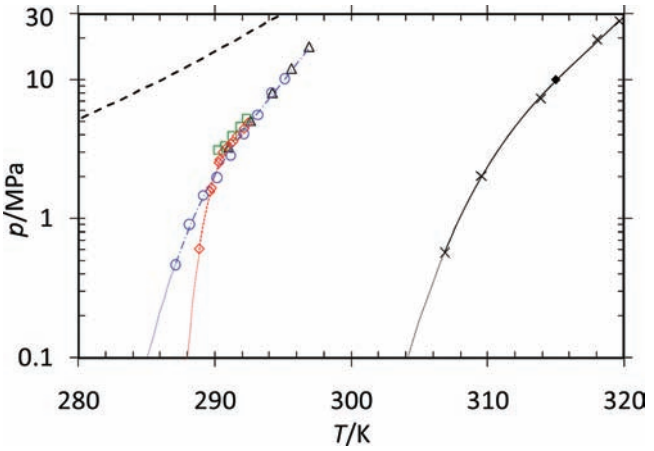

Figure 3. Three-phase p, T diagram for SCH + L + V phase equilibrium points: ×, this work, CH_4 + $(i\text{-}C_5H_{11})_4NF$ + H_2O (w = 0.315); ♦, Wang et al.,[14] CH_4 + $(i\text{-}C_5H_{11})_4NBr$ + H_2O (w = 0.36) (estimated); ○, Li et al.,[23] CH_4 + $(n\text{-}C_4H_9)_4NBr$ + H_2O (w = 0.385); Δ, Arjmandi et al.,[24] CH_4 + $(n\text{-}C_4H_9)_4NBr$ + H_2O (w = 0.3); □, Sun and Sun,[26] CH_4 + $(n\text{-}C_4H_9)_4NBr$ + H_2O (w = 0.2818); ◇, Makino et al.,[28] CH_4 + $(n\text{-}C_4H_9)_4NCl$ + H_2O (w = 0.34); ---, CH_4 + H_2O calculated using CSMGem.

Table 2. p, T SCH + L + V Equilibria Points for $(i\text{-}C_5H_{11})_4NF$ + Water (w = 0.315) + Methane, $u(T)$ = 0.02 K, $u(p)$ = 0.004 MPa

T/K	p/MPa
306.89	0.5756
309.53	2.029
313.90[a]	7.342[a]
318.00	19.680
319.68	26.653

[a] Estimated uncertainty for this point was $u(T)$ = 0.1 K, $u(p)$ = 0.01 MPa due to a singular data point before dissociation (see Supporting Information, Figure S4 and Table S8).

enclathrate methane. From Lipkowski et al.'s crystallography data the only unoccupied cages that the $(i\text{-}C_5H_{11})_4NF \cdot 27H_2O$ SCH contains are small 8-sided 4^45^4 cages, which we estimated cannot fit a methane molecule (see Supporting Information). The temperature cycling was repeated several times and helped to increase the rate of methane enclathration, as evidenced from the pressure drop. After this cycling was completed, the measurements of the next p, T phase equilibrium measurement commenced with a different initial pressure of methane.

At the completion of the five phase equilibrium measurements, the SCH was re-formed at a pressure of about 0.5 MPa following the procedures described above. The bath temperature was then set to 293 K, and the system was slowly depressurized to atmospheric pressure. The pressure cell was then opened, and the bottle end was removed. The bottle contained a solid mass of slightly yellow SCH, which was stored at room temperature (less than 298 K) for 2 days. The bottle was then heated by floating it inside a beaker of water on a heating element. Gas bubbles evolved from the SCH as it melted. A sample of the evolving gas taken by syringe and was determined to be methane by gas chromatography.

RESULTS AND DISCUSSION

Figure 2 shows an example of a series of equilibrium point measurements used to determine one CH_4 + $(i\text{-}C_5H_{11})_4NF$ + H_2O (w = 0.315) p, T SCH + L + V phase equilibrium point. The pressure and temperature of the three-phase equilibria were determined by extrapolating p, T points before and after the complete dissociation of the hydrate to the discontinuity in the p, T curve. The uncertainty in the p and T of each three-phase SCH + L + V values, considering both the uncertainty associated with equilibrium point measurements and the extrapolation, was estimated as $u(p)$ = 0.004 MPa and $u(T)$ = 0.02 K (except where otherwise noted).

The five (p, T) three-phase (SCH + L + V) values measured are displayed in Figure 3 and listed in Table 2 (note the equilibrium point measurements for each three-phase (SCH + L + V) value is listed and plotted in the Supporting Information). For comparison, the estimated three-phase (SCH + L + V) value for CH_4 + $(i\text{-}C_5H_{11})_4NBr$ + H_2O (w = 0.36, equivalent to a hydration number of 38) from Wang et al.[14] is plotted and lies very close to a curve drawn through our data (this point, at T = 315 K and p = 10.1 MPa, was estimated from the intersection of the heating and cooling curves associated with complete dissociation of the SCH in Figure 3 of Wang et al.). Also plotted in Figure 3 are the three-phase p, T phase equilibrium values for CH_4 + $(n\text{-}C_4H_9)_4NBr$ + H_2O of Li et al.[23] (w = 0.385), Arjmandi et al.[24] (w = 0.3), and Sun and Sun[26] (w = 0.2818). The slope and the shape of their curves are similar to our curve; however, our values are shifted approximately 20 K higher (we do, however, note that the data of Li et al., Arjmandi et al., and Sun and Sun may not have been recorded at the optimal mass fraction of $(n\text{-}C_4H_9)_4NBr$ for stability, which is likely to be at w = 0.320, corresponding to a hydration number of 38). Additionally the three-phase p, T phase equilibrium values for CH_4 + $(n\text{-}C_4H_9)_4NCl$ + H_2O (w = 0.34) of Makino et al.[28] are plotted in Figure 3. Their values at high pressure align closely with the literature CH_4 + $(n\text{-}C_4H_9)_4NBr$ + H_2O data but are about 2 K higher in temperature at a pressure of 0.6 MPa, presumably as the melting temperature of $(n\text{-}C_4H_9)_4NCl$ SCH is higher than $(n\text{-}C_4H_9)_4NBr$ SCH by about 2 K. The p, T slope of Makino et al.'s[28] CH_4 + $(n\text{-}C_4H_9)_4NCl$ + H_2O data is noticeably greater than both the CH_4 + $(n\text{-}C_4H_9)_4NBr$ + H_2O and CH_4 + $(i\text{-}C_5H_{11})_4NF$ + H_2O data at low pressures (p < 2 MPa).

Extrapolation of our data indicates an atmospheric pressure melting temperature of about 304.2 K; this is close to the value measured by McMullan and Jeffrey[6] of 304.4 K but lower than Lipkowski et al.'s[12] measurement of 305.6 K.

The p, T three-phase boundary for methane hydrate predicted by CSMGem[51] is also plotted in Figure 3.

At 10 MPa the dissociation temperature of CH_4 + $(i\text{-}C_5H_{11})_4NF$ + H_2O SCH is about 29 K higher than CH_4 + H_2O hydrate. At 0.1 MPa the dissociation temperature of CH_4 + $(i\text{-}C_5H_{11})_4NF$ + H_2O SCH is about 110 K higher than the CH_4 + H_2O hydrate equilibrium dissociation temperature or about 40 K higher than the methane hydrate self-preservation temperature range. This is a significant stability advantage because it is possible to store the methane in the SCH at atmospheric pressure and room temperature for at least several days. The tradeoff is the lower storage capacity offered by the SCH. As a storage material for large scale shipment, CH_4 + $(i\text{-}C_5H_{11})_4NF$ SCH may not require refrigeration for production and less or no insulation in shipment. To determine whether it could be a viable alternative to LNG or

NGH, the methane storage capacity at atmospheric pressure needs to be accurately determined and a full technical and economic analysis would need to be conducted.

■ ASSOCIATED CONTENT

Supporting Information. Figures include proton NMR spectra of $(i\text{-}C_5H_{11})_4NF$ in CD_3OD and plots of equilibrium point measurements for each three-phase (SCH + L + V) value. Tables include the chemical purities and suppliers, analytical instrument suppliers, literature three-phase (SCH+ L + V) p, T measurements and measurement methods, specifications of the experimental equipment used, and equilibrium point measurements for each three-phase (SCH + L + V) value. Also included is a size calculation for the 4^45^4 cage of $(i\text{-}C_5H_{11})_4NF \cdot 27H_2O$. This material is available free of charge via the Internet at http://pubs.acs.org.

■ AUTHOR INFORMATION

Corresponding Author
*E-mail: Thomas.Hughes@uwa.edu.au.

■ ACKNOWLEDGMENT

We appreciate Dr. Marie Squire (Chemistry Department, University of Canterbury) for assistance in collecting NMR spectra and Trevor Berry (Chemical and Process Engineering Department, University of Canterbury) for assistance with chemical preparation and GC analysis.

■ REFERENCES

(1) Fowler, D. L.; Loebenstein, D. B.; Pall; Kraus, C. A. Some Unusual Hydrates of Quaternary Ammonium Salts. *J. Am. Chem. Soc.* **1940**, *62*, 1140–1142.

(2) Beurskens, G.; Jeffrey, G. A.; McMullan, R. K. Polyhedral Clathrate Hydrates .VI. Lattice Type and Ion Distribution in Some New Peralkyl Ammonium, Phosphonium, and Sulfonium Salt Hydrates. *J. Chem. Phys.* **1963**, *39*, 3311–3315.

(3) Bonamico, M.; McMullan, R. K.; Jeffrey, G. A. Polyhedral Clathrate Hydrates. III. Structure of Tetra N-Butyl Ammonium Benzoate Hydrate. *J. Chem. Phys.* **1962**, *37*, 2219–2231.

(4) Feil, D.; Jeffrey, G. A. Polyhedral Clathrate Hydrates .II. Structure of Hydrate of Tetra Iso-Amyl Ammonium Fluoride. *J. Chem. Phys.* **1961**, *35*, 1863–1873.

(5) Jeffrey, G. A.; McMullan, R. K. Polyhedral Clathrate Hydrates . IV. Structure of Tri N-Butyl Sulfonium Fluoride Hydrate. *J. Chem. Phys.* **1962**, *37*, 2231–2239.

(6) McMullan, R.; Jeffrey, G. A. Hydrates of the Tetra n-Butyl and Tetra i-Amyl Quaternary Ammonium Salts. *J. Chem. Phys.* **1959**, *31*, 1231–1234.

(7) McMullan, R. K.; Jeffrey, G. A.; Bonamico, M. Polyhedral Clathrate Hydrates .V. Structure of Tetra-N-Butyl Ammonium Fluoride Hydrate. *J. Chem. Phys.* **1963**, *39*, 3295–3310.

(8) Aladko, L. S.; Dyadin, Y. A.; Rodionova, T. V.; Terekhova, I. S. Clathrate Hydrates of Tetrabutylammonium and Tetraisoamylammonium Halides. *J. Struct. Chem.* **2002**, *43*, 990–994.

(9) Alekseev, V. I.; Gatilov, Y. V.; Polyanskaya, T. M.; Bakakin, V. V.; Dyadin, Y. A.; Gaponenko, L. A. Characteristic Features of the Production of the Hydrate Framework Around the Hydrophobic-Hydrophillic Unit in the Crystal Structure of the Clathrate Tri-n-butylphosphine Oxide 34.5-Hydrate. *J. Struct. Chem.* **1982**, *23*, 395–399.

(10) Dyadin, Y. A.; Udachin, K. A. Clathrate Polyhydrates of Peralkylonium Salts and Their Analogs. *J. Struct. Chem.* **1987**, *28*, 394–432.

(11) Gaponenko, L.; Solodovnikov, S. F.; Dyadin, Y. A.; Aladko, L. S.; Polyanskaya, T. N. Crystallographic Study of Tetra-n-butylammonium Bromide Polydrates. *J. Struct. Chem.* **1984**, *25*, 157–159.

(12) Lipkowski, J.; Suwinska, K.; Rodionova, T. V.; Udachin, K. A.; Dyadin, Y. A. Phase and X-ray Study of Clathrate Formation in the Tetraisoamylammonium Fluoride-Water System. *J. Inclusion Phenom.* **1994**, *17*, 137–148.

(13) Shimada, W.; Shiro, M.; Kondo, H.; Takeya, S.; Oyama, H.; Ebinuma, T.; Narita, H. Tetra-n-butylammonium Bromide-Water (1/38). *Acta Crystallogr., Sect. C: Cryst. Struct. Commun.* **2005**, *61*, O65–O66.

(14) Wang, W. X.; Carter, B. O.; Bray, C. L.; Steiner, A.; Bacsa, J.; Jones, J. T. A.; Cropper, C.; Khimyak, Y. Z.; Adams, D. J.; Cooper, A. I. Reversible Methane Storage in a Polymer-Supported Semi-Clathrate Hydrate at Ambient Temperature and Pressure. *Chem. Mater.* **2009**, *21*, 3810–3815.

(15) Davidson, D. W. Clathrate Hydrates. In *Water in Crystalline Hydrates; Aqueous Solutions of Simple Nonelectrolytes*; Franks, F., Ed.; Water: A Comprehensive Treatise; Plenum: New York, 1973; Vol. 2, pp 115−234.

(16) Jeffrey, G. A. Hydrate Inclusion Compounds. In *Inclusion Compounds*; Atwood, J. L., Davies, J. E. D., MacNicol, D. D., Eds.; Academic Press: London, U.K., 1984; Vol. 1, pp 135−190.

(17) Sloan, E. D.; Koh, C. A. *Clathrate Hydrates of Natural Gases*, 3rd ed.; Chemical Industries; Taylor & Francis CRC Press: Boca Raton, FL, 2007.

(18) Stupin, D. Y.; Stravitnaya, O. S. The Sorption of Sulphur Dioxide By the Clathrate Hydrates of Tetrabutylammonium Bromide and Acetate. *Russ. J. Phys. Chem.* **1991**, *65*, 672–675.

(19) Stupin, D. Y.; Stravitnaya, O. S. The Sorption of Sulphur Dioxide By the Clathrates of Tetrabutylammonium and Tetraisopentylammonium Phthalates. *Russ. J. Phys. Chem.* **1991**, *65*, 670–672.

(20) Shimada, W.; Ebinuma, T.; Oyama, H.; Kamata, Y.; Takeya, S.; Uchida, T.; Nagao, J.; Narita, H. Separation of Gas Molecule using Tetra-n-butyl Ammonium Bromide Semi-Clathrate Hydrate Crystals. *Jpn. J. Appl. Phys., Part 2* **2003**, *42*, L129–L131.

(21) Kamata, Y.; Oyama, H.; Shimada, W.; Ebinuma, T.; Takeya, S.; Uchida, T.; Nagao, J.; Narita, H. Gas Separation Method Using Tetra-n-butylammonium Bromide Semi-Clathrate Hydrate. *Jpn. J. Appl. Phys., Part 1* **2004**, *43*, 362–365.

(22) Kamata, Y.; Yamakoshi, Y.; Ebinuma, T.; Oyama, H.; Shimada, W.; Narita, H. Hydrogen Sulfide Separation Using Tetra-n-butyl Ammonium Bromide Semi-clathrate (TBAB) Hydrate. *Energy Fuels* **2005**, *19*, 1717–1722.

(23) Li, D.-L.; Du, J.-W.; Fan, S.-S.; Liang, D.-Q.; Li, X.-S.; Huang, N.-S. Clathrate Dissociation Conditions for Methane + Tetra-n-butyl Ammonium Bromide (TBAB) + Water. *J. Chem. Eng. Data* **2007**, *52*, 1916–1918.

(24) Arjmandi, M.; Chapoy, A.; Tohidi, B. Equilibrium Data of Hydrogen, Methane, Nitrogen, Carbon Dioxide, and Natural Gas in Semi-Clathrate Hydrates of Tetrabutyl Ammonium Bromide. *J. Chem. Eng. Data* **2007**, *52*, 2153–2158.

(25) Mohammadi, A. H.; Richon, D. Phase Equilibria of Semi-Clathrate Hydrates of Tetra-n-butylammonium Bromide plus Hydrogen Sulfide and Tetra-n-butylammonium Bromide plus Methane. *J. Chem. Eng. Data* **2010**, *55*, 982–984.

(26) Sun, Z. G.; Sun, L. Equilibrium Conditions of Semi-Clathrate Hydrate Dissociation for Methane plus Tetra-n-butyl Ammonium Bromide. *J. Chem. Eng. Data* **2010**, *55*, 3538–3541.

(27) Acosta, H. Y.; Bishnoi, P. R.; Clarke, M. A. Experimental Measurements of the Thermodynamic Equilibrium Conditions of Tetra-*n*-butylammonium Bromide Semiclathrates Formed from Synthetic Landfill Gases. *J. Chem. Eng. Data* **2011**, *56*, 69–73.

(28) Makino, T.; Yamamoto, T.; Nagata, K.; Sakamoto, H.; Hashimoto, S.; Sugahara, T.; Ohgaki, K. Thermodynamic Stabilities of Tetra-n-butyl Ammonium Chloride + H_2, N_2, CH_4, CO_2, or C_2H_6 Semiclathrate Hydrate Systems. *J. Chem. Eng. Data* **2010**, *55*, 839–841.

(29) Hashimoto, S.; Sugahara, T.; Moritoki, M.; Sato, H.; Ohgaki, K. Thermodynamic stability of hydrogen+tetra-n-butyl ammonium

bromide mixed gas hydrate in nonstoichiometric aqueous solutions. *Chem. Eng. Sci.* **2008**, *63*, 1092–1097.

(30) Deschamps, J.; Dalmazzone, D. Dissociation Enthalpies and Phase Equilibrium for TBAB Semi-Clathrate Hydrates of N_2, CO_2, N_2 + CO_2 and CH_4 + CO_2. *J. Therm. Anal. Calorim.* **2009**, *98*, 113–118.

(31) Lipkowski, J.; Komarov, V. Y.; Rodionova, T. V.; Dyadin, Y. A.; Aladko, L. S. The Structure of Tetra-Butyl-Ammonium Bromide Hydrate $(C_4H_9)_4NBr \cdot 2^1/_3H_2O$. *J. Supramol. Chem.* **2002**, *2*, 435–439.

(32) Berner, D. The Marine Transport of Natural Gas In Hydrate Form. *Proceedings of the Second International Offshore and Polar Engineering Conference*, San Francisco, CA, June 14−19, 1992; International Society of Offshore and Polar Engineers: Cupertino, CA, 1992; pp 636−643.

(33) Gudmundsson, J. S.; Andersson, V.; Dugut, I.; Levik, O. I.; Mork, M. NGH on FPSO - Slurry Process and Cost Estimate. *Proceedings of the SPE Annual Technical Conference*, Houston, TX, October 3−6, 1999; Society of Petroleum Engineers: Richardson, TX, 1999.

(34) Gudmundsson, J. S.; Andersson, V.; Levik, O. I. Gas Storage and Transport Using Hydrates. *Proceedings of the Offshore Mediterranean Conference*, Ravenna, Italy, Mar 19−21, 1997; OMC SCRL: Ravenna, Italy, 1997.

(35) Gudmundsson, J. S.; Borrehaug, A. A Frozen Hydrate for Transport of Natural Gas. *Proceedings of the 2nd International Conference on Natural Gas Hydrates*, Toulouse, France, June 2−6, 1996; Institut National Polytechnique, École Nationale Supérieure Ingenieurs Genie Chimique: Toulouse, France, 1996; pp 415−422.

(36) Gudmundsson, J. S.; Børrehaug, A. Natural Gas Hydrate - An Alternative to Liquefied Natural gas. *Petrol. Rev.* **1996**, *50*, 232–235.

(37) Gudmundsson, J. S.; Graff, O. F. Hydrate Non-Pipeline Technology for Transport of Natural Gas. *Proceedings of the 22nd World Gas Conference*, Tokyo, Japan, June 1−5, 2003; International Gas Union: Oslo, Norway, 2003.

(38) Gudmundsson, J. S.; Mork, M. Stranded Gas to Hydrate for Storage and Transport. *2001 International Gas Research Conference*, Amsterdam, Netherlands, November 5−8, 2001; International Gas Union: Oslo, 2001.

(39) Gudmundsson, J. S.; Mork, M.; Graff, O. F. Hydrate Non-Pipeline Technology. *Proceedings of the 4th International Conference on Gas Hydrates*, Yokohama, Japan, May 19−23 [CDROM], 2002; Mori, Y. H., Ed.; 997−1002.

(40) Yakushev, V. S.; Istomin, V. A. Gas-Hydrates Self-Preservation Effect. In *Physics and Chemistry of Ice*; Maeno, N., Hondoh, T., Eds.; Hokkaido University Press: Sapporo, Japan, 1992; pp 136−139.

(41) Gudmundsson, J. S.; Parlaktuna, M.; Khokar, A. A. Storing Natural Gas as Frozen Hydrate. *SPE Prod. Facil.* **1994**, *9*, 69–73.

(42) Fallabella, B. J.; Vanpee, M. Experimental Determination of Gas Hydrate Equilibrium below the Ice Point. *Ind. Eng. Chem. Fundamen.* **1974**, *13*, 228–231.

(43) Stern, L. A.; Circone, S.; Kirby, K. B.; Durham, W. B. Temperature, Pressure, and Compositional Effects on Anomalous or "Self" Preservation of Gas Hydrates. *Can. J. Phys.* **2003**, *81*, 271–283.

(44) Nogami, T.; Oya, N.; Ishida, H.; Matsumoto, H. Development of Natural Gas Ocean Transportation Chain by Means of Natural Gas Hydrate (NGH). *Proceedings of the 6th International Conference on Gas Hydrates*, Vancouver, Canada, July 6−10, 2008; University of British Columbia: Vancouver, Canada, 2008.

(45) Tohidi, B.; Burgass, R. W.; Danesh, A.; Østergaard, K. K.; Todd, A. C. Improving the Accuracy of Gas Hydrate Dissociation Point Measurements. *Ann. N. Y. Acad. Sci.* **2000**, *912*, 924–931.

(46) Chapoy, A.; Anderson, R.; Tohidi, B. Low-Pressure Molecular Hydrogen Storage in Semi-clathrate Hydrates of Quaternary Ammonium Compounds. *J. Am. Chem. Soc.* **2007**, *129*, 746–747.

(47) Chapoy, A.; Gholinezhad, J.; Tohidi, B. Experimental Clathrate Dissociations for the Hydrogen plus Water and Hydrogen plus Tetrabutylammonium Bromide plus Water Systems. *J. Chem. Eng. Data* **2010**, *55*, 5323–5327.

(48) Lee, S.; Lee, Y.; Park, S.; Seo, Y. Phase Equilibria of Semiclathrate Hydrate for Nitrogen in the Presence of Tetra-n-butylammonium Bromide and Fluoride. *J. Chem. Eng. Data* **2010**, *55*, 5883–5886.

(49) Li, S. F.; Fan, S. S.; Wang, J. Q.; Lang, X. M.; Wang, Y. H. Semiclathrate Hydrate Phase Equilibria for CO_2 in the Presence of Tetra-n-butyl Ammonium Halide (Bromide, Chloride, or Fluoride). *J. Chem. Eng. Data* **2010**, *55*, 3212–3215.

(50) Oyama, H.; Shimada, W.; Ebinuma, T.; Kamata, Y.; Takeya, S.; Uchida, T.; Nagao, J.; Narita, H. Phase diagram, latent heat, and specific heat of TBAB semiclathrate hydrate crystals. *Fluid Phase Equilib.* **2005**, *234*, 131–135.

(51) Ballard, A. L. A Non-ideal Hydrate Solid Solution Model for a Multi-phase Equilibria Program. *Ph.D Thesis*, Colorado School of Mines, Golden, CO, 2002.

(52) Tse, J. S. Thermal Expansion of the Clathrate Hydrates of Ethylene Oxide and Tetrahydrofuran. *J. Phys. Colloques* **1987**, *48*, C1–543-C1−549.

(53) Handa, Y. P.; Hawkins, R. E.; Murray, J. J. Calibration and Testing of a Tian-Calvet Heat-Flow Calorimeter. Enthalpies of Fusion and Heat Capacities for Ice and Tetrahydrofuran Hydrate in the Range 85 to 270 K. *J. Chem. Thermodyn.* **1984**, *16*, 623–32.

(54) Lemmon, E. W.; Huber, M. L.; McLinden, M. O. *NIST Standard Reference Database 23: Reference Fluid Thermodynamic and Transport Properties-REFPROP, 7.1*; National Institute of Standards and Technology: Gaithersburg, MD, 2003.